IEEE Access
Multidisciplinary | Rapid Review | Open Access Journal

Received June 4, 2020, accepted June 15, 2020, date of publication June 18, 2020, date of current version July 8, 2020.

Digital Object Identifier 10.1109/ACCESS.2020.3003329

Performance Improvement for Wireless Sensors Networks by Adopting Hybrid Subcarrier Intensity Modulation Over Exponentiated Weibull Turbulence Channels

YI WU[1], YUAN HAO[1], HONGZHAN LIU[1,2], LIN ZHAO[1], (Graduate Student Member, IEEE), TING JIANG[1], (Graduate Student Member, IEEE), DONGMEI DENG[1,2], AND ZHONGCHAO WEI[1,2]

[1]Guangdong Provincial Key Laboratory of Nanophotonic Functional Materials and Devices, South China Normal University, Guangzhou 510006, China
[2]School of Information and Optoelectronic Science and Engineering, South China Normal University, Guangzhou 510006, China

Corresponding author: Hongzhan Liu (lhzscnu@163.com)

This work was supported by the National Natural Science Foundation of China under Grant 61875057, Grant 61475049, and Grant 61774062.

ABSTRACT We conduct a research on free space optical (FSO) communication system that is applied for transmission in wireless sensor networks (WSN), which is based on the hybrid pulse position modulation-binary phase shift keying-subcarrier intensity modulation (PPM-BPSK-SIM) undergoes novel Exponentiated Weibull fading channels. When battery-charged sensor transmission nodes with limited energy is transmitted, it is vital to study the performance of the transmission link. We have derived the exact joint probability function of the transmission link when the atmospheric turbulence and pointing errors are considering. On the basis of them, the unconditional average bit error rate (BER) for hybrid PPM-BPSK-SIM is derived, then the closed expression of the outage probability and the average channel capacity are also derived. Research results indicates that increasing the receiver aperture by aperture averaging effect can distinctly improve the performance of the link. Additionally, for any circumstances of atmospheric turbulence and pointing errors, by combining the utilization of hybrid PPM-BPSK-SIM modulation and symbol with average length greater than eight, the average BER performance can be conspicuously enhanced. The outage probability and average channel capacity of the FSO link are jointly affected by atmospheric turbulence and pointing error, and optimization strategies in different scenarios are given by our research.

INDEX TERMS Wireless sensor networks (WSN), free space optical (FSO), exponentiated Weibull fading channels, pointing errors, PPM-BPSK-SIM, BER, average symbol length.

I. INTRODUCTION

Wireless sensor networks (WSN) have raised extensive research in recent years due to their advantages of small size and low cost. However, WSN has inherent problems such as low bandwidth and limited battery supply energy. Meanwhile, the increase in number of sensor nodes has brought serious problems such as shortage of spectrum resources [1], [2]. The application of free space optical (FSO) communication to WSN transmission will bring considerable benefits, such as larger bandwidth, higher security, smaller size of transmitting and receiving antennas, and higher transmission efficiency [3]–[6]. However, when the WSN is deployed in actual application scenarios, the FSO link as its transmission medium will be affected by atmospheric turbulence, which causes problems such as fluctuations in the signal intensity of the receiving information center, as well as interference generated by the pointing error between the receiving antenna and beam center caused by incomplete coincidence [7], [8]. The high bit error rate (BER) and other problems caused by the above two phenomena deteriorate the transmission efficiency of WSN, and the limited battery supply life is seriously affected [9], [10]. Therefore, it is necessary to study the performance indicators such as the

The associate editor coordinating the review of this manuscript and approving it for publication was Hongwei Du.

average BER of FSO communication links under interference in WSN in order to improve the operating efficiency of the entire networks.

Malaga model mentioned in many studies is relatively applicable for effects on weak, moderate and strong turbulent conditions [11], [12]. In the actual transmission link, the aperture average effect will be an economical and simple technique to make up the fading created by atmospheric turbulence, more specifically by increasing the aperture of the receiver, the power fluctuations created by atmospheric turbulence and other factors may be averaged to various apertures to compensate the transmission loss of the FSO link, which can also be seen as an ordinary method of spatial diversity when the receiver aperture is greater than the fading correlation length [13]–[15]. Especially in the short-distance transmission commonly used in WSN, the Gaussian beam wave model with limited beam width is more suited to describe the propagation characteristics of the transmitted light wave, and the receiving aperture is not negligible for the beam width at the destination. At this time, using the traditional Malaga model, the accuracy of it is verified by the simulation data of infinite plane waves and spherical waves and consequently, the receiving aperture on the WSN cannot be well discussed. Therefore, the FSO link model used in this study adopts the newly proposed Exponentiated Weibull (EW) distribution model, which is defined by simulation of Gaussian beam wave as well as comprehensive experimental data over various turbulence conditions. Besides EW distribution model also can better fit the actual experimental data from weak to strong atmosphere turbulence under the aperture averaging effect than the Malaga models mentioned in [16]–[18], particularly for the dot-shaped aperture. Especially in the WSN communication link with high accuracy requirements, it is attached great importance to select the EW model to study the average SNR, outage probability and the channel capacity of the link.

As the most generalized model for the FSO link, Malaga model has been widely studied, the performance of Malaga link considering pointing error is studied [19], [20] has investigated average capacity of Malaga link with pointing errors when adaptive transmission is adopted [21] proposed a novel indirect diffused light FSO system in vehicular networks, high speed data transmission is realized. A balanced detector in FSO link with optical fiber is presented when multiple phase shift keying (MPSK) is adopted and the performance of BER has been studied [22]. Owning to the above advantages, the research of EW distribution has received extensive attention these years. The average BER of the EW distribution adopting BPSK modulation, subcarrier BPSK modulation, and PPM modulation without considering the pointing error have been separately studied [23]–[27]. The performance of LDPC code in FSO link under EW channel is studied in [28]. The latest research has conducted the research of OOK modulation and polarization shift keying (PolSK) considering the pointing error [29]. The BER performance of Radio Frequency (RF)/FSO has been studied in [30], while both of receiving aperture and pointing errors don't seem to have been thoroughly studied. Based on previous studies, BPSK is widely used in FSO links as a low BER binary modulation, but little research has been done on the improvement of high-order modulation and hybrid subcarrier intensity modulation for communication systems, let alone that the receiver aperture is considered. Based on this, we studied the performance of the EW model using various hybrid PPM-BPSK-SIM modulation [31]–[33], atmospheric turbulence with pointing errors is taken into account. We derived the unconditional BER of various PPM-BPSK-SIM when intensity modulation/direct detection (IM/DD) is employed at the receiver [34], meanwhile closed solution of the outage probability and average channel capacity are also obtained, and simulation analysis shows that the adoption of hybrid subcarrier intensity modulation undoubtedly improve the FSO link transmission in wireless sensor networks [35].

The structure of this paper is as follows. The system model and channel model of FSO communication link in wireless sensor network will be described in Section II. We will derive the outage probability, the unconditional BER and the average channel capacity of the FSO link respectively by Meijer's G function in Section III. Results of numerical simulations realized by MATLAB, and inductive analysis of simulation results will be shown in Section IV. Section V contains concluding remarks.

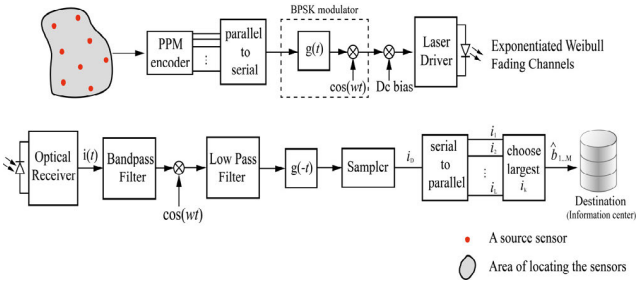

FIGURE 1. Structure diagram of the system model.

II. SYSTEM AND CHANNEL MODELS

The system model of transmission from the sensor collection source to the destination information center in a certain area is shown in Fig. 1. The data information of the sensor collection source is modulated by PPM encoder and transmission by parallel-to-serial conversion to BPSK subcarrier modulator, after adding the DC bias and digital-to-analog, the subcarrier modulated signal is got, which will be loaded onto the light wave through laser deriver. The light wave carrying the information is transmitted to the Exponentiated Weibull turbulence channel through an optical antenna, which will be received by a certain aperture optical received. Then the received signal is converted into the electrical signal and processed by the filter and sampler, the signal is divided into parallel low rate signal by serial-to-parallel conversion, finally the output information can be obtained in destination. When the information of the sensor collection source

is transmitted by different modulation methods, we use the simple structure and more practical IM / DD technology at the receiver end. The signal generated at the destination is:

$$y = Rhx + n. \tag{1}$$

where h defined as the accumulated channel gain, which is indicated as $h = h_a h_p h_l$. h_a is expressed as the fading caused by turbulence, and h_p indicates the fading caused by the pointing error. h_l stands for a deterministic fading caused by atmospheric attenuation, which can be set to a constant of 1 without loss of generality. R is the corresponding coefficient of the photodetector. x is a BPSK subcarrier intensity modulated signal, the average power of which is P. n is independent of the Gaussian white noise with a mean of 0 and a variance of σ_n^2. Here we can give the definition of the instantaneous signal-to-noise ratio (SNR) at the receiving end as:

$$\gamma = \frac{R^2 P^2 h^2}{2\sigma_n^2} = \overline{\gamma} h^2. \tag{2}$$

where $\overline{\gamma} = \frac{R^2 P^2}{2\sigma_n^2}$ is the averages SNR in FSO link.

Considering the aperture average effect, the channels of the FSO link follow the Exponential Weibull (EW) distribution can be given by [16]:

$$f_{h_a}(h_a) = \frac{\alpha\beta}{\eta}\left(\frac{h_a}{\eta}\right)^{\beta-1} \exp\left[-\left(\frac{h_a}{\eta}\right)^{\beta}\right]\left\{1-\exp\left[-\left(\frac{h_a}{\eta}\right)^{\beta}\right]\right\}^{\alpha-1}. \tag{3}$$

where $\alpha, \beta > 0$ are defined as the shape parameters, $\gamma > 0$ is defined as scale parameter, both of them can be calculated by the (20)-(22) in [18]. By the relation of $f_{\gamma_a}(\gamma_a) = \frac{1}{2\sqrt{\gamma\overline{\gamma}}} f_{h_a}\left(\sqrt{\frac{\gamma}{\overline{\gamma}}}\right)$, the Probability Density Function (PDF) of the instantaneous SNR is obtained by

$$f_{\gamma_a}(\gamma_a) = \frac{\alpha\beta}{2\overline{\gamma}\eta^{\beta}} (\eta t)^{\beta-2} \exp\left(-t^{\beta}\right)\left[1-\exp\left(-t^{\beta}\right)\right]^{\alpha-1}. \tag{4}$$

where $t = \sqrt{\gamma / \left(\overline{\gamma}\eta^2\right)}$.

The pointing error is due to the slight shaking that will cause the center of the beam spot and the receiver aperture to be at different points. The PDF of intensity scintillation fading affected by the point error can be given by [36]:

$$f_{h_p}(h_p) = \frac{\rho^2}{A_0^{\rho^2}} h_p^{\rho^2-1} \quad 0 \le h_p \le A_0. \tag{5}$$

where A_0 is received optical power when radial displacement is 0, given as $A_0 = [erf(v)]^2$, where $erf(\bullet)$ is error function. ρ denotes the ratio of the equivalent beam waist radius and jitter standard deviation at the receiving end which represented as $\rho = \omega_{eq} / (2\sigma_s)$. σ_s denotes the jitter standard deviation, the larger the σ_s is, the greater the beam jitter is, and means the stronger the pointing error is. ω_{eq} stands for the equivalent beam width that can be expressed as $\omega_{eq} = \omega\sqrt{\sqrt{\pi} erf(v) / 2v \exp\left(-v^2\right)}$ and $v = \sqrt{\pi/2}(a/\omega)$, a denotes the radius of optical receiver, ω is the beam width at distance z.

The joint error model is solved as follows:

$$\begin{aligned} f_h(h) &= \frac{1}{h_a}\int f_{h_p}\left(\frac{h}{h_a}\right) \bullet f_{ha}(h_a)\, dh_a \\ &= \frac{\rho^2}{A_0^{\rho^2} h_a}\left(\frac{h}{h_a}\right)^{\rho^2-1} f_{ha}(h_a)\, dh_a, \quad 0 \le h \le A_0 h_a \end{aligned} \tag{6}$$

where $\Gamma(\bullet)$ stands for the Gamma function, $G(\bullet)$ represents the Meijer's G function [37]. Utilizing Formula of Gamma Function $\int_z^{\infty} e^{-t} t^{a-1} dt = \Gamma(a,x) = G_{1\ 2}^{2\ 0}\left(x\middle|\begin{matrix}1\\0\ a\end{matrix}\right)$, $\exp(x) = G_{0\ 1}^{1\ 0}\left(-x\middle|\begin{matrix}-\\0\end{matrix}\right)$ and the Newton's General Binomial Theorem Formula:

$$\left\{1-\exp\left[-\left(\frac{h_a}{\eta}\right)^{\beta}\right]\right\}^{\alpha-1} = \sum_{i=0}^{\infty} \frac{\Gamma(\delta+1)}{i!\Gamma(\delta-i+1)} \exp\left[-i\left(\frac{h_a}{\eta}\right)^{\beta}\right]. \tag{7}$$

The PDF of the instantaneous SNR in FSO link combines turbulence fading and pointing error is derived as follows:

$$f_{\gamma}(\gamma) = \frac{\alpha\rho^2}{(\eta A_0)^{\rho^2}\gamma}\left(\sqrt{\frac{\gamma}{\overline{\gamma}}}\right)^{\rho^2} \sum_{i=0}^{\infty} \frac{(-1)^i \Gamma(\alpha)}{i!\Gamma(\alpha-i)(1+i)^{1-\frac{\rho^2}{\beta}}} G_{1\ 2}^{2\ 0}\left[\frac{1+i}{(\eta A_0)^{\beta}}\sqrt{\frac{\gamma}{\overline{\gamma}}}^{\beta}\middle|\begin{matrix}1\\0\quad 1-\frac{\rho^2}{\beta}\end{matrix}\right]. \tag{8}$$

The Cumulative Probability Function (CDF) of the instantaneous SNR is given by integration [16]:

$$\begin{aligned} F_{\gamma}(\gamma) &= \int_0^{\gamma} f_{\gamma}(\gamma) d\gamma \\ &= \frac{\alpha\rho^2}{\beta(\eta A_0)^{\rho^2}}\left(\sqrt{\frac{\gamma}{\overline{\gamma}}}\right)^{\rho^2} \sum_{i=0}^{\infty} \frac{(-1)^i \Gamma(\alpha)}{i!\Gamma(\alpha-i)(1+i)^{1-\frac{\rho^2}{\beta}}} G_{2\ 3}^{2\ 1}\left[\frac{1+i}{(\eta A_0)^{\beta}}\left(\sqrt{\frac{\gamma}{\overline{\gamma}}}\right)^{\beta}\middle|\begin{matrix}1-\frac{\rho^2}{\beta} & 1\\ 0 & 1-\frac{\rho^2}{\beta} & 1-\frac{\rho^2}{\beta}\end{matrix}\right]. \end{aligned} \tag{9}$$

III. PERFORMAN ANALYSIS

A. OUTAGE PROBABILITY

Outage probability represents the probability that the instantaneous SNR is lower than the preset threshold value, γ_{th}, that is $P_{out} = \Pr(\gamma \le \gamma_{th})$. The outage probability of the link is

derived by:

$$P_{out} = \frac{\alpha\rho^2}{\beta(\eta A_0)^{\rho^2}}\left(\sqrt{\frac{\gamma_{th}}{\overline{\gamma}}}\right)^{\rho^2}\sum_{i=0}^{\infty}\frac{(-1)^i\Gamma(\alpha)}{i!\Gamma(\alpha-i)(1+i)^{1-\frac{\rho^2}{\beta}}} G_{2\ 3}^{2\ 1}\left[\frac{1+i}{(\eta A_0)^{\beta}}(\sqrt{\frac{\gamma_{th}}{\overline{\gamma}}})^{\beta}\Big|\begin{matrix}1-\frac{\rho^2}{\beta} & 1 \\ 0 & 1-\frac{\rho^2}{\beta} \end{matrix}\ \ 1-\frac{\rho^2}{\beta}\right]. \quad (10)$$

B. AVERAGE BIT ERROR RATE

There are many kinds of modulation methods that can be applied to transmission system of WSN, which can generate a considerable difference in performance of system due to their different properties, for example, spectrum efficiency and bandwidth efficiency. However, it is certain that the average BER of the system is the simplest and the most intuitive criterion to assess the quality of different modulation schemes. As mentioned above, BPSK, as a simple and low BER modulation method, has been widely concerned in WSN system. Reference [38] studied the performance of BPSK, and we take it as a comparative basis.

The newly proposed PPM-BPSK-SIM combines two traditional modulation methods, PPM and BPSK-SIM. That is, the information symbols are modulated to parallel signal by the PPM encoder, after being converted, the high rate serial signal is transmitted to the BPSK modulator [39]. For L-ary pulse position modulation (LPPM), one data symbol is composed by L time slots, among which only one time slot is valid while the others are zero. Therefore, the average length of the symbol is L, the conditional BER for various PPM is $P_{e,LPPM} = \frac{1}{2}erfc\left(\frac{1}{2}\sqrt{\frac{1}{4}\gamma L\log_2 L}\right)$ [24], [40]–[42]. According to (2) and (8) in [31], the deterministic relationship of the conditional BER between LPPM and LPPM–BPSK–SIM is obtained, squaring up the relationship of $Q(x) = \frac{1}{2}erfc\left(\frac{x}{\sqrt{2}}\right)$, the conditional BER of the hybrid LPPM-BPSK-SIM can be given by $P_{e,LPPM-BPSK-SIM} = Q\left(\frac{1}{4}\sqrt{\gamma L\log_2 L}\right)$.

The unconditional BER of various PPM can be derived by:

$$P_{LPPM} = \int_0^{\infty} f_{\gamma}(\gamma)P_{e,LPPM}d\gamma = \int_0^{\infty}\frac{\alpha\rho^2}{2(\eta A_0)^{\rho^2}\gamma}\left(\sqrt{\frac{\gamma}{\overline{\gamma}}}\right)^{\rho^2}\sum_{i=0}^{\infty}\frac{(-1)^i\Gamma(\alpha)}{i!\Gamma(\alpha-i)(1+i)^{1-\frac{\rho^2}{\beta}}} G_{1\ 2}^{2\ 0}\left[\frac{1+i}{(\eta A_0)^{\beta}}\sqrt{\frac{\gamma}{\overline{\gamma}}}^{\beta}\Big|\begin{matrix}1 \\ 0\end{matrix}\ \ 1-\frac{\rho^2}{\beta}\right] * erfc\left(\frac{1}{2}\sqrt{\frac{1}{4}\gamma L\log_2 L}\right)d\gamma. \quad (11)$$

Utilizing the relationship of Meijer's G function: $erfc(x) = \frac{1}{\sqrt{\pi}}G_{1\ 2}^{2\ 0}\left[x^2\Big|\begin{matrix}1 \\ 0\ \frac{1}{2}\end{matrix}\right]$ and (2.24.1.1) in [43], the closed form formula for LPPM can be obtained:

For hybrid LPPM-BPSK-SIM empathically, the unconditional BER can be derived by:

$$P_{LPPM-BPSK-SIM} = \int_0^{\infty} f_{\gamma}(\gamma)P_{e,LPPM-BPSK-SIM}d\gamma = \int_0^{\infty}\frac{\alpha\rho^2}{2(\eta A_0)^{\rho^2}\gamma}\left(\sqrt{\frac{\gamma}{\overline{\gamma}}}\right)^{\rho^2}\sum_{i=0}^{\infty}\frac{(-1)^i\Gamma(\alpha)}{i!\Gamma(\alpha-i)(1+i)^{1-\frac{\rho^2}{\beta}}} G_{1\ 2}^{2\ 0}\left[\frac{1+i}{(\eta A_0)^{\beta}}\sqrt{\frac{\gamma}{\overline{\gamma}}}^{\beta}\Big|\begin{matrix}1 \\ 0\end{matrix}\ \ 1-\frac{\rho^2}{\beta}\right] * Q\left(\frac{1}{4}\sqrt{\gamma L\log_2 L}\right)d\gamma. \quad (13)$$

The closed form of the above formula can be expressed as:

In (12) and (14) as shown at the bottom of the next page, $\sigma = \frac{L\log_2 L}{16}, \mu = \eta A_0\sqrt{\overline{\gamma}}, \tau = \frac{\rho^2}{\beta}$. By utilizing the Meijer's G function represented in [43], l and k are integer numbers that suffice the relationship $l/k = \beta$. The $\Delta(m,n)$ is a sequence denoted as $\Delta(m,n) = \left(\frac{n}{m}\right), \left(\frac{n+1}{m}\right), \ldots, \left(\frac{n+m+1}{m}\right)$. As an example, $\Delta(4,2)$ can be expressed as $\Delta(4,2) = \frac{2}{4}, \frac{3}{4}, \frac{4}{4}, \frac{5}{4}$.

C. AVERAGE CHANNEL CAPACITY

The accurate definition of the average channel capacity can be given in [44], [45] which is $\overline{C} = E\left[B\log_2(1+\gamma)\right]$. $E(\bullet)$ refers to the mathematical expectation operator. Based on this, the normalized average channel capacity of the FSO link can be obtained as:

$$< C_{ave} > = \int_0^{\infty}\log_2(1+\gamma)f_{\gamma}(\gamma)d\gamma = \frac{1}{\ln 2}\int_0^{\infty}\ln(1+\gamma)f_{\gamma}(\gamma)d\gamma. \quad (15)$$

Utilizing $\ln(1+x) = G_{2\ 2}^{1\ 2}\left(x\Big|\begin{matrix}1 & 1 \\ 1 & 0\end{matrix}\right)$ [37] and (2.24.1.1) in [46], the mathematical closed analytical formula of the above formula can be obtained (16) as shown at the bottom of the next page. where $\mu = \eta A_0\sqrt{\overline{\gamma}}, l$ and k are integer numbers that suffice the relationship $l/k = \beta$. The $\Delta(m,n)$ is a sequence denoted as $\Delta(m,n) = \left(\frac{n}{m}\right), \left(\frac{n+1}{m}\right), \ldots, \left(\frac{m+n-1}{m}\right)$.

IV. NUMERICAL RESULTS AND DISCUSSION

This Section will use the mathematical closed formulas obtained in Section III to analyze the performance of the FSO link under the hybrid various PPM-BPSK-SIM, such as outage probability, BER, and average channel capacity.

Therefore, we use the novel EW distribution model to quantitatively describe atmospheric turbulence, the interference caused by pointing errors is considered, and the receiver employs IM/DD to obtain the performance of the FSO transmission link. Therefore, taking the average aperture effect into account, we set the receiver aperture to $D = 200mm, 100mm, 50mm$. Besides, we set turbulence model parameter $\sigma_R = 0.32, 2.22, 15.9$ in correspondence with weak, moderate and strong turbulence intensity, and the wavelength is 1550nm. In (7)-(15), the closed form is given by the form of infinite series, when $i = 100$ is selected in the calculation, the closed type basically converges, meanwhile the truncation error of the closed type is less than 10^{-10}. Considering the similarity of the formulas, we choose some different cases in each picture for Monte Carlo simulation, the simulation results are in closely approximate with the analytic results, which validate the correctness of our formulas. The parameters of EW distribution under different conditions are listed in TABLE 1 [16], and TABLE 2 shows the parameters of the link [47], [48].

Setting the SNR threshold as $\gamma_{th} = 10dB$, the outage probability of the FSO transmission link against average SNR is displayed in Fig. 2 and Fig. 3 when considering turbulent fading and pointing error. Clearly, the descent in the turbulence intensity causes the decrease of the outage probability, and when σ_s decreases, which means the pointing error decreases, the outage probability drops significantly. When the pointing error is low, the average SNR required for strong turbulence is 6dB higher than that for weak turbulence in order to achieve the outage probability lower than $P_{\text{out}} = 10^{-3}$, and it

TABLE 1. The parameters of EW distribution for different conditions.

Receive Aperture	Turbulence	α	β	η
D=100mm	Weak	1.84	7.11	0.99
	Moderate	3.52	2.15	0.76
	Strong	4.82	1.07	0.47
D=200mm	Moderate	2.15	5.40	0.96
D=50mm		4.65	1.17	0.51

TABLE 2. The parameters of the FSO link.

Parameter	Value
Wavelength (λ=1440nm) propagating path(z)	5000m
Corresponding beam width(ω) at z	0.02mrad*z
Corresponding jitter standard deviation(σ_s)	20cm or 30cm

$$P_{LPPM} = \frac{-\alpha\sigma\tau}{2\sqrt{\pi}\mu^{\rho^2}} \frac{k^{-\tau-0.5}}{(2\pi)^{\frac{k+l-2}{2}}} \sigma^{-\rho-1} \sum_{i=0}^{\infty} \frac{(-1)^i \Gamma(\alpha)}{i!\Gamma(\alpha-i)(1+i)^{1-\tau}} \cdot G_{2k+3l}^{2k+l\ \ k+2l} \left[\left(\frac{l}{\sigma}\right)^l \left(\frac{1+i}{k\mu^\beta}\right)^k \middle| \begin{matrix} \Delta(k,1-\tau) & \Delta(l,1-\rho) & \Delta(l,\frac{1}{2}-\rho) & \Delta(l,-\rho) & \Delta(k,1) \\ \Delta(k,0) & \Delta(k,1-\tau) & \Delta(l,1-\rho) & \Delta(l,-\rho) & \end{matrix} \right]. \quad (12)$$

$$P_{LPPM-BPSK-SIM} = \frac{-\alpha\sigma\tau}{4\sqrt{\pi}\mu^{\rho^2}} \frac{k^{-\tau-0.5}}{(2\pi)^{\frac{k+l-2}{2}}} \left(\frac{\sigma}{2}\right)^{-\rho-1} \sum_{i=0}^{\infty} \frac{(-1)^i \Gamma(\alpha)}{i!\Gamma(\alpha-i)(1+i)^{1-\tau}} \cdot G_{2k+3l}^{2k+l\ \ k+2l} \left[\left(\frac{2l}{\sigma}\right)^l \left(\frac{1+i}{k\mu^\beta}\right)^k \middle| \begin{matrix} \Delta(k,1-\tau) & \Delta(l,1-\rho) & \Delta(l,\frac{1}{2}-\rho) & \Delta(l,-\rho) & \Delta(k,1) \\ \Delta(k,0) & \Delta(k,1-\tau) & \Delta(l,1-\rho) & \Delta(l,-\rho) & \end{matrix} \right]. \quad (14)$$

$$\begin{aligned} < C_{ave} > &= \frac{\alpha\rho^2}{\mu^{\rho^2}\ln 2} \sum_{i=0}^{\infty} \frac{(-1)^i\Gamma(\alpha)}{i!\Gamma(\alpha-i)(1+i)^{1-\tau}} \int_0^{\infty} \gamma^{\frac{\rho^2}{2}-1} \\ &\quad G_{2\ 2}^{1\ 2}\left[\gamma \middle| \begin{matrix} 1 & 1 \\ 1 & 0 \end{matrix}\right] G_{1\ 2}^{2\ 0}\left[\frac{(1+i)}{\mu^\beta}\gamma^{\frac{\beta}{2}} \middle| \begin{matrix} 1 & \\ 0 & 1-\tau \end{matrix}\right] d\gamma \\ &= \frac{\alpha\rho^2}{\beta\mu^{\rho^2}\ln 2} \frac{k^{-\tau-0.5}}{l*(2\pi)^{l+k/2-1.5}} \sum_{i=0}^{\infty} \frac{(-1)^i\Gamma(\alpha)}{i!\Gamma(\alpha-i)(1+i)^{1-\tau}} \\ &\quad \bullet G_{k+2l\ \ 2k+2l}^{2k+2l\ \ l} \left[\left(\frac{1+i}{k\mu^\beta}\right)^k \middle| \begin{matrix} \Delta(k,-\tau) & \Delta(l,1-\tau) & \Delta(k,1) & \\ \Delta(k,0) & \Delta(k,1-\tau) & \Delta(l,-\frac{\rho^2}{2}) & \Delta(l,-\frac{\rho^2}{2}) \end{matrix} \right]. \end{aligned} \quad (16)$$

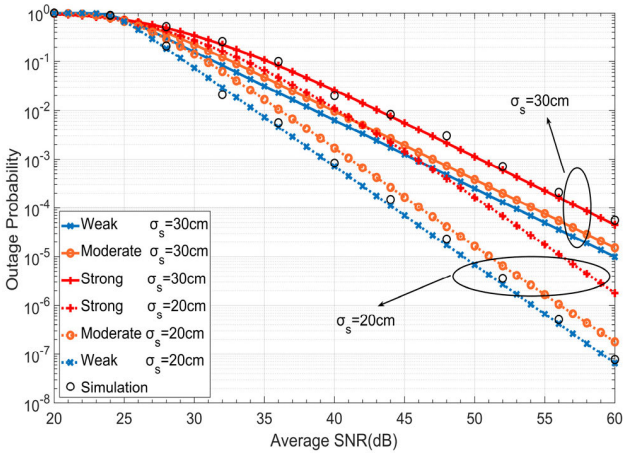

FIGURE 2. **Outage probability against average SNR for different turbulence intensities and pointing errors, where threshold of the FSO link is $\gamma_{th} = 10$dB.**

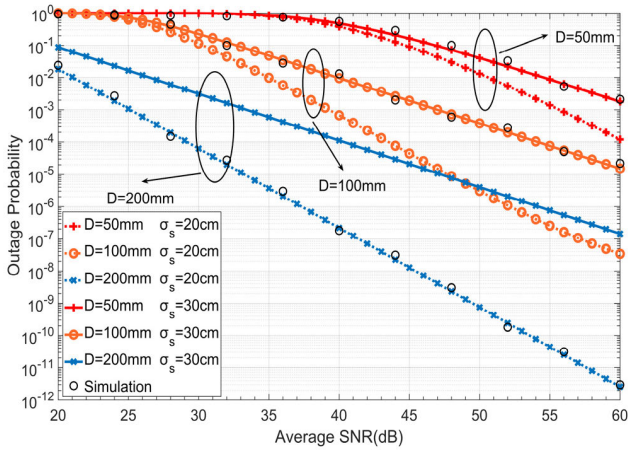

FIGURE 3. **Outage probability against average SNR for different receive apertures and pointing errors, where threshold of the FSO link is $\gamma_{th} = 10$dB.**

becomes 4dB while the pointing error is high. Such research has revealed that when the pointing error is low, the outage probability of the transmission link is more influenced by turbulence, and artificially reducing the pointing error, such as correcting the symmetry of the transmitter and receiver or reducing the jitter of the transmitted beam can weaken the influence of uncontrollable atmospheric turbulence fluctuations on the outage performance of FSO link. Besides, under strong turbulent conditions, the atmospheric fading is severe, and the impact of the change in pointing errors on the outage performance will become smaller at this time, therefore it is not cost-effective to correct the pointing error to produce such enhancement in performance. When considering the receiver aperture, larger receiving aperture brings better outage performance. When the receiver with larger aperture is adopted in the system, the influence of pointing error on the system will be overcome to some extent. When the average SNR is fixed to 60dB, the decrease in pointing error will lead to the changes in outage probability of three systems with different apertures sizes (D = 50mm, 100mm and 200mm), which are $1.8*10^{-3}$ to $1.2*10^{-4}$, $1.5*10^{-5}$ to $3.4*10^{-8}$ and $1.4*10^{-7}$ to $2.6*10^{-12}$. That is, the outage performance of the system with large receiving aperture is more sensitive to the change of pointing errors, which means it is more reasonable to adjust the alignment of the receiving and transmitting antennas to obtain the outage probability required by the actual WSN's communication system.

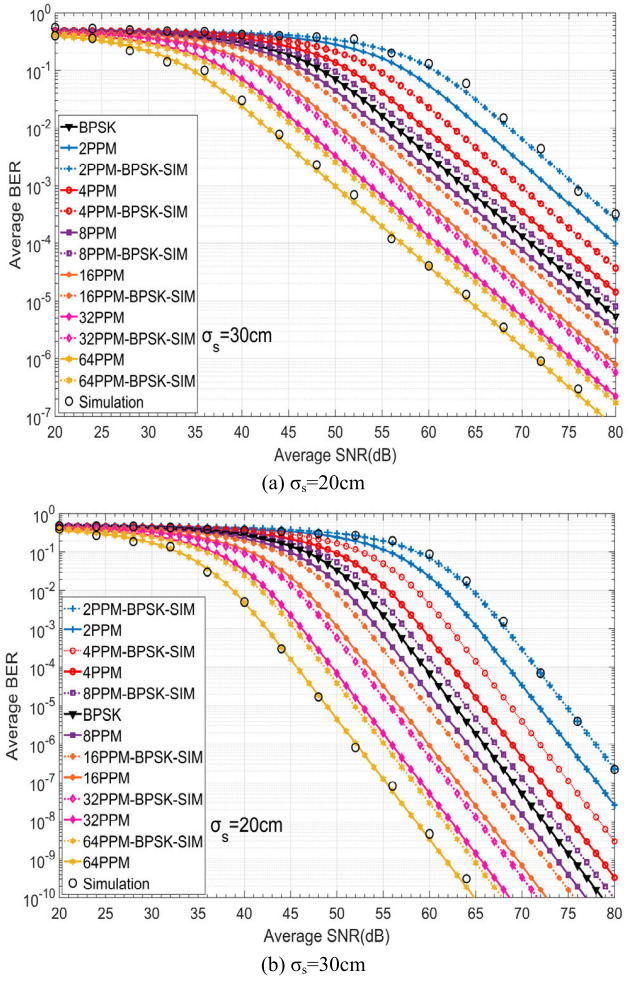

FIGURE 4. **Average BER against average SNR under weak turbulence with different pointing errors. (a) The corresponding jitter standard deviation is $\sigma_s = 20$cm. (b) The corresponding jitter standard deviation is $\sigma_s = 30$cm.**

Fig. 4 (a) and Fig. 4 (b) respectively study the performance of various LPPM and hybrid various LPPM-BPSK-SIM under weak turbulence conditions with the two pointing error strengths. We can conclude that increasing the value L will significantly improve the BER performance of the link. LPPM will outperform BPSK in BER when value L is greater than four, while adopting LPPM-BPSK-SIM, the required L needs to be greater than eight. Through a comparative study on the change of the pointing error intensity, it is found that the two modulation methods are close to improvement brought by the traditional BPSK modulation.

However, increasing L will reduce the bit error rate at the expense of band efficiency, so we focus our research on L valued at 8 or 16.

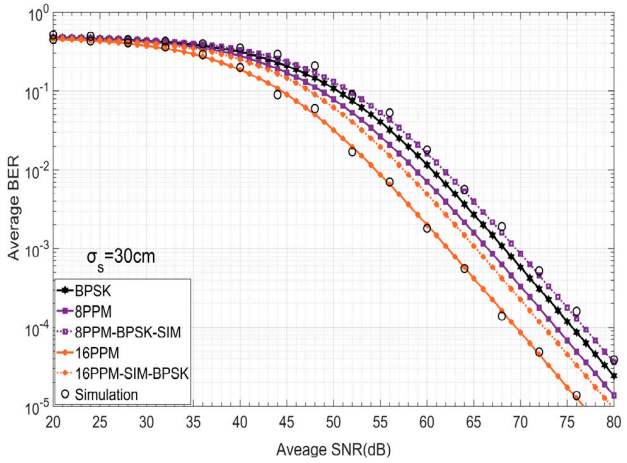

FIGURE 5. Average BER against average SNR under strong turbulence with high pointing error, the corresponding jitter standard deviation is σ_s = 30cm. Turbulence parameters are $\alpha = 4.82$, $\beta = 1.07$ and $\eta = 0.47$.

Fig. 5 investigates the BER performance of high pointing error and strong turbulent fading conditions. It is discovered that in the case where the channel quality is very poor, the conclusions obtained are consistent with the case where the channel quality is better, that is, L must be greater than four or eight, respectively, so that the BER performance of the two modulation methods outperforms than the traditional BPSK system, which is also consistent with the conclusion in Fig. 4 (a) and Fig. 4 (b). Then Fig. 6 compares the performance of the hybrid modulation system under strong and weak turbulence with low pointing errors. When the intensity of turbulence rises, the average BER will increase significantly. In order to reduce the average BER from 10^{-3} to 10^{-6}, the link adopting 16PPM-BPSK-SIM needs to increase the average SNR by 14dB under strong turbulence, while only 9.5dB of increase in the average SNR is needed under weak turbulence. Meanwhile, when adopting the 16PPM-BPSK-SIM in transmission link, in order to make the BER lower than 10^{-3}, the average SNR under weak turbulent conditions will be 7dB lower than under strong turbulent conditions, in both cases, the BER of 8PPM-BPSK-SIM is tremendously close to that of BPSK.

Considering that the aperture averaging effect has a certain impact on improving the link's performance, the influence of the receiver aperture size on the performance of BER will be studied next. Fig. 7 depicts the average BER in a large aperture receiver (D = 200mm) against the average SNR. The simulation results show that when the receiver aperture is increased to D = 200mm, the link's performance is conspicuously improved. Meanwhile, the improvement effect of LPPM and LPPM-BPSK-SIM compared with traditional BPSK is the same as when D = 100mm. It is worth noting that when the pointing error is low ($\sigma_s = 20cm$), increasing

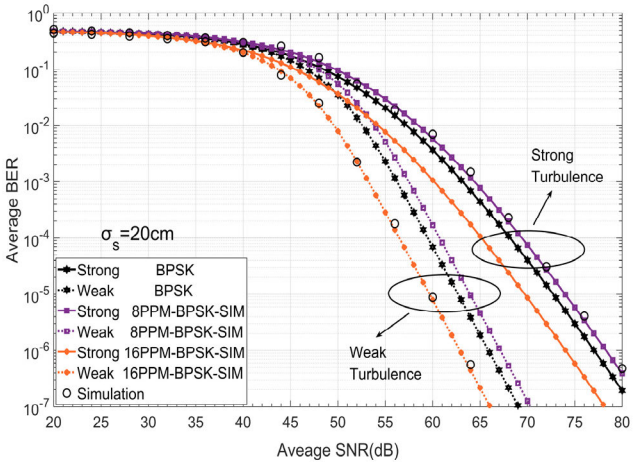

FIGURE 6. Average BER against average SNR under different turbulences with low pointing error, the corresponding jitter standard deviation is σ_s = 20cm. Turbulence parameters are $\alpha = 4.82$, $\beta = 1.07$, $\eta = 0.47$ and $\alpha = 1.84$, $\beta = 7.11$ and $\eta = 0.99$, respectively, under strong or weak turbulence condition.

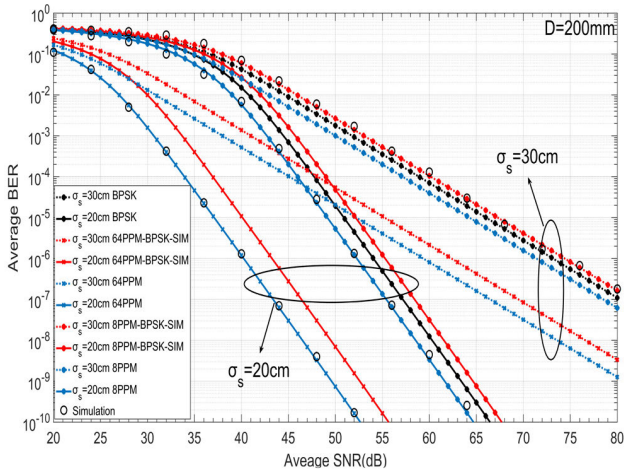

FIGURE 7. Average BER against average SNR under moderate turbulence with different pointing errors. Receiver with large aperture (D = 200mm) is adopted. Turbulence parameters are $\alpha = 2.15$, $\beta = 5.40$, $\eta = 0.96$, while the corresponding jitter standard deviation are σ_s = 20cm or σ_s = 30cm.

the value L of the two various modulation methods will distinctly improve the performance of the link, and under the same average SNR, the BER of 64PPM-BPSK-SIM is only $6.25*10^{-5}$ of 8PPM-BPSK-SIM, while under high pointing error ($\sigma_s = 30cm$), it drops to $6.67*10^{-3}$, which means high pointing error will impair the effect of the value L. The research results show that in the high pointing error ($\sigma_s = 30cm$) situation, the cost-effectiveness of reducing the average BER by increasing the average symbol length will decrease, and the rate of the average BER decreasing with the increase of the average SNR will become slow, which leads to the flat decline of the average BER. Consequently, the link must be under the conditions with high average BER to obtain ideal average BER performance.

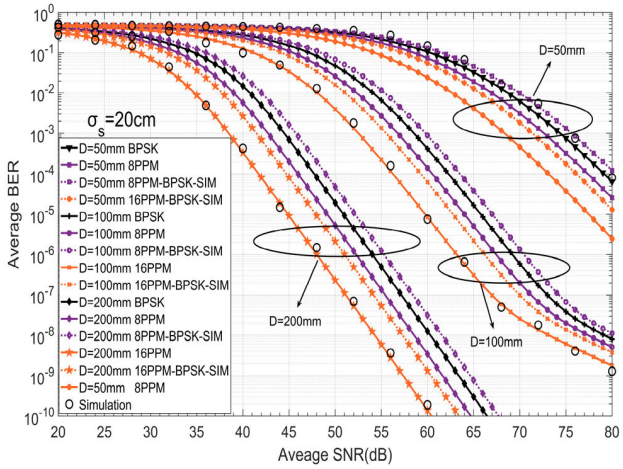

FIGURE 8. Average BER against average SNR under moderate turbulence with different receive apertures. Turbulence parameters are $\alpha = 4.65$, $\beta = 1.17$, $\eta = 0.51$; $\alpha = 3.52$, $\beta = 2.15$, $\eta = 0.76$ and $\alpha = 2.15$, $\beta = 5.40$, $\eta = 0.96$, respectively, when the receive aperture is 50mm, 100mm and 200mm, while the corresponding jitter standard deviation is $\sigma_s = 20$cm.

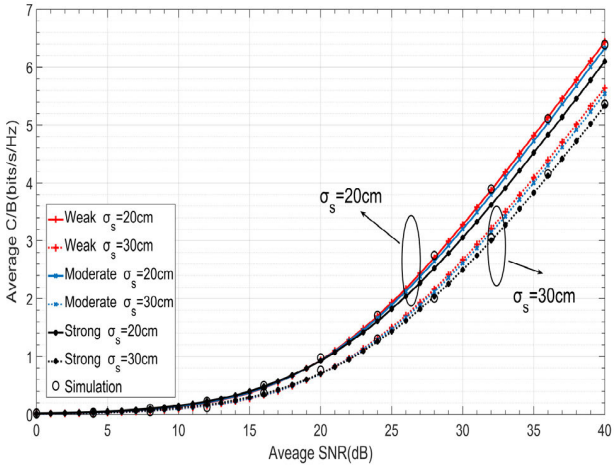

FIGURE 9. Average channel capacity against average SNR for different turbulence intensities and different pointing error parameters.

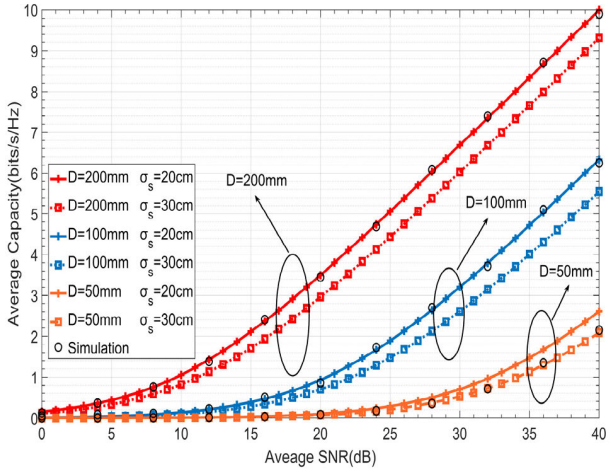

FIGURE 10. Average channel capacity against average SNR for different receive apertures and different pointing error parameters.

Fig. 8 compares the influence of the receiver aperture size on the system. It can be found that when the receiving aperture rises, the average BER performance of the system is significantly improved. For example, when the system adopts 8PPM-BPSK-SIM or 16PPM-BPSK-SIM, in order to achieve average BER of 10^{-6}, the receiver aperture of D = 200mm will bring a gain of 15.2dB in the average SNR over the receiver aperture of D = 100mm. On the other hand, under three different receiving apertures, LPPM and LPPM-BPSK-SIM have the same improvement in the average BER performance of BPSK system, but larger receiving aperture makes change in average BER more sensitive to the average SNR. When adopting 16PPM-BPSK-SIM, in order to reduce the average BER from 10^{-3} to 10^{-6}, the increase needed in the average SNR is 9.4dB and 10.8dB for receiver with D = 200mm and D = 100mm, respectively, which indicates that the large aperture receiver system is more suitable for communication under the complex channel environment. Therefore, in different turbulence, pointing errors and receiver aperture conditions, the hybrid various PPM-BPSK-SIM may conspicuously enhance the BER performance of the link. Compared with the BSPK system, the improvement of hybrid PPM-BPSK-SIM also exists even under conditions of strong turbulence and severe pointing errors.

Fig. 9 and Fig. 10 depict the average channel capacity under different turbulence intensities, pointing errors and receiving apertures, respectively. The results show that the average channel capacity increases with the decrease of turbulence intensity and pointing error and the increase of receiving apertures. Under strong turbulent conditions, when the σ_s changes from 20cm to 30cm and the average SNR is 40dB, the average channel capacity of the FSO link increases by 0.8 bit/s/Hz, the fluctuation of the corresponding jitter standard deviation in this range seems to have a more significant impact on the average channel capacity. When the pointing error is fixed, the channel capacity will decrease slightly as the turbulence intensity increases. We have concluded that lower pointing error causes higher average capacity, then pointing errors may make the influence of turbulence on capacity performance more serious. Besides, when the receiving aperture increases, the channel capacity of the link will be significantly improved compared with the effect caused by pointing errors. When the average SNR is 40 dB, the channel capacity gain caused by the decrease of pointing error is approximately 0.7bits/s/Hz under the three sizes of receiving apertures (D = 50mm, D = 100mm and D = 200mm). The above study shows that when the receiving aperture is fixed, the channel capacity of the link cannot be improved obviously by adjusting the pointing errors artificially. Specifically, in WSN applications where high transmission speed is required, the receiver with larger aperture can better meet the actual communication needs according to the averaging aperture effect.

V. CONCLUSION

In summary, we have studied the performance of the FSO link in the wireless sensor networks when the hybrid LPPM-BPSK-SIM is adopted. The channel conditions of the transmission link comprehensively consider the fading caused by the atmospheric turbulence and pointing error that undergoes novel Exponentiated Weibull model. Based on the precise Meijer's G function, the closed mathematical form of the joint error model of the link is derived, from which the unconditional BER of the transmission link is obtained. In addition, the performance of the outage probability and channel capacity are also investigated on the basis of the joint error model above.

The results of our research prove that the average BER performance could be improved by adopting hybrid LPPM-BPSK-SIM. Moreover, the exact improvement effect has a close relationship with the average symbol length. More specifically, when the average symbol length increases, the average BER of the link will decrease significantly. Especially when it is greater than eight, the average BER of the link will be better than adopting BPSK. Even in the condition of strong turbulence and high pointing errors, adopting hybrid LPPM-BPSK-SIM can significantly improve the link's performance stably. On the other hand, pointing error will obviously worsen the link quality, which will impair the enhancement in BER performance generated by the increase of L, as well as causing the average BER to decrease more slowly as the average SNR increases. Owing to the aperture averaging effect, when the receiver aperture is increased, it can obviously compensate the system fading caused by strong turbulence and high pointing error, so that the system performance is significantly improved. The outage probability and average channel capacity of the link seem sensitive to the pointing error, and the pointing errors will make the impact of atmospheric turbulence more serious. However, the joint utilization of hybrid LPPM-BPSK-SIM and aperture averaging effect can effectively improve the transmission efficiency of wireless sensor networks under any conditions of turbulence and pointing errors. In our work, we study the outage probability, average BER and average channel capacity of FSO link. On the premise of fully considering the uncontrollable factor of atmospheric turbulence, we propose the practical strategy, that is, to adjust the changeable pointing error parameters and receiver aperture in the actual scene, which supplies a conception for the deployment of FSO in WSN.

APPENDIX

The following abbreviations are used in this manuscript:

FSO	Free space optical
WSN	Wireless sensor network
BER	Bit error rate
AA	Aperture average
EW	Exponentiated Weibull
OP	Outage probability
PDF	Probability density function
IM/DD	Intensity-modulation/direct-detection
SNR	Signal-to-noise power ratio
MGF	Meijer's G function
CDF	Cumulative distribution function

REFERENCES

[1] I. F. Akyildiz, W. Su, Y. Sankarasubramaniam, and E. Cayirci, "Wireless sensor networks: A survey," *Comput. Netw.*, vol. 38, no. 4, pp. 393–422, 2002.
[2] S. Debnath and A. Hossain, "Network coverage in interference limited wireless sensor networks," *Wireless Pers. Commun.*, vol. 109, no. 1, pp. 139–153, Nov. 2019.
[3] L. Stotts, B. Stadler, and G. Lee, "Free space optical communications: Coming of age," presented at the SPIE Int. Soc. Opt. Eng., San Francisco, CA, USA, 2008.
[4] D. Wu, X. Sun, and N. Ansari, "An FSO-based drone assisted mobile access network for emergency communications," *IEEE Trans. Netw. Sci. Eng.*, early access, Sep. 2019, doi: 10.1109/TNSE.2019.2942266.
[5] G. Aarthi and G. R. Reddy, "Average spectral efficiency analysis of FSO links over turbulence channel with adaptive transmissions and aperture averaging," *Opt. Commun.*, vol. 410, pp. 896–902, Mar. 2018.
[6] Z. Gu, J. Zhang, Y. Ji, L. Bai, and X. Sun, "Network topology reconfiguration for FSO-based Fronthaul/Backhaul in 5G+ wireless networks," *IEEE Access*, vol. 6, pp. 69426–69437, 2018.
[7] A. A. Farid and S. Hranilovic, "Outage capacity optimization for free-space optical links with pointing errors," *J. Lightw. Technol.*, vol. 25, no. 7, pp. 1702–1710, Jul. 2007.
[8] N. Ansari, D. Wu, and X. Sun, "FSO as backhaul and energizer for drone-assisted mobile access networks," *ICT Express*, vol. 6, no. 2, pp. 139–144, Jun. 2020.
[9] K. A. Balaji and K. Prabu, "Performance evaluation of FSO system using wavelength and time diversity over Malaga turbulence channel with pointing errors," *Opt. Commun.*, vol. 410, pp. 643–651, Mar. 2018.
[10] M. A. Esmail, H. Fathallah, and M.-S. Alouini, "On the performance of optical wireless links over random foggy channels," *IEEE Access*, vol. 5, pp. 2894–2903, 2017.
[11] F. Vetelino, C. Young, and L. Andrews, "Fade statistics for Gaussian beam waves in moderate-to-strong turbulence," *Appl. Opt.*, vol. 46, pp. 3780–3789, Jan. 2007.
[12] J. Garrido-Balsells, A. Jurado-Navas, J. F. Paris, M. del Castillo Vázquez, and A. Puerta-Notario, "Novel formulation of the $\mathcal{M}$ model through the generalized-K distribution for atmospheric optical channels," *Opt. Express*, vol. 23, pp. 6345–6358, Mar. 2015.
[13] N. Perlot and D. Fritzsche, "Aperture-averaging—Theory and measurements," *Proc. SPIE*, vol. 5338, pp. 233–242, Jun. 2004.
[14] F. Vetelino, C. Young, L. Andrews, and J. Recolons, "Aperture averaging effects on the probability density of irradiance fluctuations in moderate-to-strong turbulence," *Appl. Opt.*, vol. 46, pp. 108–2099, May 2007.
[15] M.-A. Khalighi, N. Schwartz, N. Aitamer, and S. Bourennane, "Fading reduction by aperture averaging and spatial diversity in optical wireless systems," *IEEE/OSA J. Opt. Commun. Netw.*, vol. 1, no. 6, pp. 580–593, Nov. 2009.
[16] R. Barrios and F. Dios, "Exponentiated Weibull distribution family under aperture averaging for Gaussian beam waves," *Opt. Express*, vol. 20, no. 12, pp. 13055–13064, Jun. 2012.
[17] P. K. Sharma, A. Bansal, P. Garg, T. A. Tsiftsis, and R. Barrios, "Performance of FSO links under exponentiated Weibull turbulence fading with misalignment errors," *Nature*, vol. 433, no. 7021, pp. 57–59, 2015.
[18] R. Barrios and F. Dios, "Exponentiated weibull model for the irradiance probability density function of a laser beam propagating through atmospheric turbulence," *Opt. Laser Technol.*, vol. 45, pp. 13–20, Feb. 2013.
[19] I. S. Ansari, F. Yilmaz, and M.-S. Alouini, "Performance analysis of free-space optical links over Málaga ($\mathcal{M}$) turbulence channels with pointing errors," *IEEE Trans. Wireless Commun.*, vol. 15, no. 1, pp. 91–102, Jan. 2016.
[20] M. Smilić, Z. Nikolić, D. Milić, P. Spalević, and S. Panić, "Comparison of adaptive algorithms for free space optical transmission in Málaga atmospheric turbulence channel with pointing errors," *IET Commun.*, vol. 13, no. 11, pp. 1578–1585, Jul. 2019.

[21] Y. Kaymak, S. Fathi-Kazerooni, and R. Rojas-Cessa, "Indirect diffused light free-space optical communications for vehicular networks," *IEEE Commun. Lett.*, vol. 23, no. 5, pp. 814–817, May 2019.
[22] H. Yao, X. Ni, C. Chen, B. Li, X. Feng, X. Liu, Z. Liu, S. Tong, and H. Jiang, "Performance analysis of MPSK FSO communication based on the balanced detector in a fiber-coupling system," *IEEE Access*, vol. 7, pp. 84197–84208, 2019.
[23] R. Barrios and F. Dios, "Probability of fade and BER performance of FSO links over the exponentiated Weibull fading channel under aperture averaging," presented at the SPIE Int. Soc. Opt. Eng., San Francisco, CA, USA, 2012.
[24] T. Y. Elganimi, "Performance comparison between OOK, PPM and PAM modulation schemes for free space optical (FSO) communication systems: Analytical study," *Int. J. Comput. Appl.*, vol. 79, no. 11, pp. 22–27, Oct. 2013.
[25] W. O. Popoola and Z. Ghassemlooy, "BPSK subcarrier intensity modulated free-space optical communications in atmospheric turbulence," *J. Lightw. Technol.*, vol. 27, no. 8, pp. 967–973, Apr. 15, 2009.
[26] X. Yi, Z. Liu, and P. Yue, "Average BER of free-space optical systems in turbulent atmosphere with exponentiated Weibull distribution," *Opt. Lett.*, vol. 37, pp. 5142–5144, Dec. 2012.
[27] X. Yi and M. Yao, "Free-space communications over exponentiated Weibull turbulence channels with nonzero boresight pointing errors," *Opt. Express*, vol. 23, no. 3, pp. 2904–2917, Feb. 2015.
[28] X. Liu, P. Wang, T. Liu, Y. Li, L. Guo, and H. Tian, "ABER performance of LDPC-coded OFDM free-space optical communication system over exponentiated weibull fading channels with pointing errors," *IEEE Photon. J.*, vol. 9, no. 4, pp. 1–13, Aug. 2017.
[29] L. Zhang, J. Wang, P. Xiang, J. Zhao, H. Zhou, J. Zheng, H. Zhang, Y. Shen, and T. Pu, "Performance analysis of circle polarization shift keying modulation over the exponentiated weibull distribution," *Opt. Rev.*, vol. 27, no. 1, pp. 39–44, Feb. 2020.
[30] E. Erdogan, N. Kabaoglu, I. Altunbas, and H. Yanikomeroglu, "On the error probability of cognitive RF-FSO relay networks over Rayleigh/EW fading channels with primary-secondary interference," *IEEE Photon. J.*, vol. 12, no. 1, pp. 1–13, Feb. 2020.
[31] M. Faridzadeh, A. Gholami, and S. Rajbhandari, "Hybrid PPM-BPSK subcarrier intensity modulation for free space optical communications," presented at the 16th Eur. Conf. Netw. Opt. Commun. (NOC), London, U.K., 2011.
[32] M. Faridzadeh, A. Gholami, Z. Ghassemlooy, and S. Rajbhandari, "Hybrid pulse position modulation and binary phase shift keying subcarrier intensity modulation for free space optics in a weak and saturated turbulence channel," (in English), *JOSAA*, vol. 29, no. 8, pp. 1680–1685, Aug. 2012.
[33] X. Song, F. Yang, and J. Cheng, "Subcarrier intensity modulated optical wireless communications in atmospheric turbulence with pointing errors," *IEEE/OSA J. Opt. Commun. Netw.*, vol. 5, no. 4, pp. 349–358, Apr. 2013.
[34] T. Song, M.-W. Wu, and P.-Y. Kam, "Mitigation of the background radiation for free-space optical IM/DD systems," *IEEE Commun. Lett.*, vol. 22, no. 2, pp. 292–295, Feb. 2018.
[35] S. Yadav and V. Kumar, "Optimal clustering in underwater wireless sensor networks: Acoustic, EM and FSO communication compliant technique," *IEEE Access*, vol. 5, pp. 12761–12776, 2017.
[36] D. K. Borah and D. G. Voelz, "Pointing error effects on free-space optical communication links in the presence of atmospheric turbulence," *J. Lightw. Technol.*, vol. 27, no. 18, pp. 3965–3973, Sep. 15, 2009.
[37] M. Trott. *The Wolfram Functions Site*. Accessed: Mar. 3, 2020. [Online]. Available: http://functions.wolfram.com/
[38] P. Wang, L. Zhang, L. Guo, F. Huang, T. Shang, R. Wang, and Y. Yang, "Average BER of subcarrier intensity modulated free space optical systems over the exponentiated Weibull fading channels," (in English), *Opt. Express*, vol. 22, no. 17, pp. 20828–20841, Aug. 2014.
[39] M. Faridzadeh, A. Gholami, Z. Ghassemlooy, and A. Gatri, "BPSK-SIM-PPM modulation for free space optical communications," in *Proc. 7th Int. Symp. Telecommun. (IST)*, Toronto, ON, Canada, 2014, pp. 794–798.
[40] X. Yi, Z. Liu, P. Yue, and T. Shang, "BER performance analysis for M-ary PPM over Gamma-Gamma atmospheric turbulence channels," in *Proc. 6th Int. Conf. Wireless Commun. Netw. Mobile Comput. (WiCOM)*, Chengdu, China, 2010, pp. 1–4.
[41] M. Faridzadeh, A. Gholami, Z. Ghassemlooy, and S. Rajbhandari, "Hybrid 2-PPM-BPSK-SIM with the spatial diversity for free space optical communications," presented at the 8th Int. Symp. Commun. Syst., Netw. Digit. Signal Process. (CSNDSP), Poznan, Poland, Jul. 2012.
[42] S. Trisno, "Design and analysis of advanced free space optical communication systems," Ph.D. dissertation, Dept. Elect. Comput. Eng., Univ. Maryland, College Park, MD, USA, 2006.
[43] A. P. Prudnikov, Y. Brychkov, and O. I. Marichev, *Integrals and Series: More Special Functions*, vol. 3. Moscow, Russia: Gordon and Breach Science Publishers, 1989.
[44] A. Annamalai, R. C. Palat, and J. Matyjas, "Estimating ergodic capacity of cooperative analog relaying under different adaptive source transmission techniques," in *Proc. IEEE Sarnoff Symp.*, Priceton, NJ, USA, Apr. 2010, pp. 1–5.
[45] C. Si, Y. Zhang, Y. Wang, J. Wang, and J. Jia, "Average capacity for non-Kolmogorov turbulent slant optical links with beam wander corrected and pointing errors," *Optik*, vol. 123, no. 1, pp. 1–5, Jan. 2012.
[46] D. Zwillinger and V. Moll, *Table of Integrals, Series, and Products*, 8th ed. Boston, MA, USA: Academic, 2014.
[47] Z. Ghassemlooy, W. Popoola, and S. Rajbhandari, *Optical Wireless Communications: System and Channel Modelling with MATLAB*. Boca Raton, FL, USA: CRC Press, 2019.
[48] R. Bosu and S. Prince, "Link budget profile for infrared FSO link with aerial platform," presented at the Opt. Wireless Technol., Singapore, 2020.

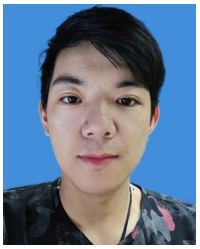

YI WU received the bachelor's degree from South-Central University for Nationalities, China, in 2018. He is currently pursuing the master's degree with the School for Information and Optoelectronic Science and Engineering, South China Normal University. His current research interest includes optical communication in free space.

YUAN HAO received the bachelor's degree from South China Agricultural University, China, in 2018. He is currently pursuing the master's degree in information and optoelectronic science and engineering with South China Normal University. His current research interests include vortex light research and image recognition.

HONGZHAN LIU received the Ph.D. degree from the Graduate School of Chinese Academy of Sciences. He is currently a Professor in information and optoelectronic science and engineering with South China Normal University, where he is also a member of the Guangdong Provincial Key Laboratory of Nanophotonic Functional Materials and Devices. His research interests include satellite-ground laser communication, precision measurement, sensing, and the Internet-of-Things technology.

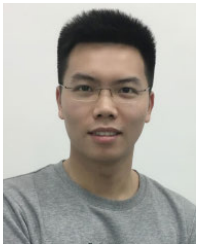

LIN ZHAO (Graduate Student Member, IEEE) was born in Nanchong, Sichuan, China, in 1994. He received the bachelor's degree from Shanxi Datong University, in 2016. He is currently pursuing the master's degree with the School for Information and Optoelectronic Science and Engineering, South China Normal University. His current research interests include optical communication, vortex, and free-space optical communications.

TING JIANG (Graduate Student Member, IEEE) received the bachelor's degree from the Hubei University of Economics, China, in 2017. She is currently pursuing the master's degree in information and optoelectronic science and engineering with South China Normal University. Her current research interest includes optical communication in free space.

DONGMEI DENG received the Ph.D. degree from South China Normal University, in 2010. She is currently a Professor with the School of Information and Optoelectronic Science and Engineering, South China Normal University. She has published more than 90 peer-reviewed articles, a number of book chapters, and patents. Her research interests include optical beams, pulses, and pulsed beams, atmospheric and oceanic turbulence, and plasmonic structures.

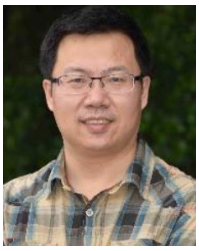

ZHONGCHAO WEI received the Ph.D. degree from Sun Yat-sen University, China. He is currently a Professor in information and optoelectronic science and engineering with South China Normal University, where he is also a member of the Guangdong Provincial Key Laboratory of Nanophotonic Functional Materials and Devices. His research interests include micronano photonics, metamaterials and metamaterials, and surface plasma optics.